

Transient ferromagnetic-like state mediating ultrafast reversal of antiferromagnetically coupled spins

I. Radu^{1,2}, K. Vahaplar¹, C. Stamm², T. Kachel², N. Pontius², H. A. Dürr^{2,3}, T. A. Ostler⁴, J. Barker⁴, R. F. L. Evans⁴, R. W. Chantrell⁴, A. Tsukamoto^{5,6}, A. Itoh⁵, A. Kirilyuk¹, Th. Rasing¹ & A. V. Kimel¹

Ferromagnetic or antiferromagnetic spin ordering is governed by the exchange interaction, the strongest force in magnetism^{1–4}. Understanding spin dynamics in magnetic materials is an issue of crucial importance for progress in information processing and recording technology. Usually the dynamics are studied by observing the collective response of exchange-coupled spins, that is, spin resonances, after an external perturbation by a pulse of magnetic field, current or light. The periods of the corresponding resonances range from one nanosecond for ferromagnets down to one picosecond for antiferromagnets. However, virtually nothing is known about the behaviour of spins in a magnetic material after being excited on a timescale faster than that corresponding to the exchange interaction (10–100 fs), that is, in a non-adiabatic way. Here we use the element-specific technique X-ray magnetic circular dichroism to study spin reversal in GdFeCo that is optically excited on a timescale pertinent to the characteristic time of the exchange interaction between Gd and Fe spins. We unexpectedly find that the ultrafast spin reversal in this material, where spins are coupled antiferromagnetically, occurs by way of a transient ferromagnetic-like state. Following the optical excitation, the net magnetizations of the Gd and Fe sublattices rapidly collapse, switch their direction and rebuild their net magnetic moments at substantially different timescales; the net magnetic moment of the Gd sublattice is found to reverse within 1.5 picoseconds, which is substantially slower than the Fe reversal time of 300 femtoseconds. Consequently, a transient state characterized by a temporary parallel alignment of the net Gd and Fe moments emerges, despite their ground-state antiferromagnetic coupling. These surprising observations, supported by atomistic simulations, provide a concept for the possibility of manipulating magnetic order on the timescale of the exchange interaction.

Understanding the physics of non-equilibrium magnetic phenomena is crucial for the understanding of ultrafast magnetization dynamics. This research field started with the seminal observation of subpicosecond demagnetization in ferromagnetic nickel⁵ by a 60-fs laser pulse, and was subsequently fuelled by a plethora of fundamentally intriguing ultrafast magnetic phenomena⁶. To study this transient regime of spin dynamics where novel coupling phenomena can emerge, one faces two challenges: (1) how to probe the response of one magnetic moment relative to another; and (2) how to bring the moments out of equilibrium on a timescale corresponding to the exchange interaction.

Ferrimagnetic materials are ideal candidates with which to address both these problems. First, in contrast to elementary ferromagnets, such as Fe, Ni or Co, and typical antiferromagnets like NiO where all the spins are equivalent, ferrimagnets consist of two (or more) non-equivalent and antiferromagnetically coupled spin sublattices⁷. This non-equivalence of the sublattices in combination with an

element-specific detection technique like X-ray magnetic circular dichroism (XMCD) allows us to ‘colour’ spins in the magnet and to probe the response of one moment relative to another. Second, ultrafast heating of a ferrimagnet over its compensation point in an external magnetic field allows the initiation of the fastest spin reversal reported so far^{8,9}. The simplest ferrimagnet, consisting of two collinear magnetic sublattices, may possess a magnetization compensation temperature denoted as T_M . T_M is the result of the different temperature dependences of the two sublattice magnetizations, and represents the point where the magnetizations of these two antiparallel-coupled sublattices are equal and cancel each other. Heating the ferrimagnetic Gd(FeCo) alloy with subpicosecond laser pulses over T_M in an external magnetic field triggers the reversal of the FeCo sublattice within 700 fs (ref. 9). Looking at the Gd sublattice during ultrafast spin reversal of its neighbour Fe would thus be a promising approach to generate and study a state with decoupled behaviour and different dynamics of the two sublattices.

As a model system for such studies, we have used thin films of the amorphous ferrimagnetic alloy Gd₂₅Fe_{65.6}Co_{9.4}, where Gd and FeCo represent two antiferromagnetically coupled collinear magnetic sublattices¹⁰. For simplicity, in the following we focus on the behaviour of the Gd and Fe moments and ignore the small percentage of Co in the transition metal sublattice (Supplementary Information). In order to probe the magnetizations of the two sublattices independently, we used the element-specific XMCD technique. The XMCD measurements were performed in transmission for a fixed X-ray light helicity and opposite orientations of the external magnetic field of ± 0.5 T. The photon energy of the X-ray light was tuned at the Fe L₃ and at the Gd M₅ absorption edges in order to measure their magnetic response separately. In Fig. 1 we show the results of static XMCD measurements as a function of magnetic field measured below and above T_M . The XMCD signals at the Fe and Gd edges reveal the respective sign change of the hysteresis loops on heating the alloy above T_M . Therefore, the data in Fig. 1 confirm that XMCD serves as an element-specific probe of spins in this rare earth-transition metal alloy (see also Supplementary Information).

In order to trigger ultrafast spin dynamics in this alloy, we initiated the reversal of the magnetizations of the two sublattices by ultrafast heating of the sample above T_M using a linearly polarized 60-fs laser pulse with photon energy of 1.55 eV. The dynamics of the Fe and Gd magnetic moments were independently probed using 100-fs soft X-ray pulses^{11,12} (see Supplementary Information section 1). Figure 2 shows the results of time-resolved measurements of the dynamics of the Fe and Gd sublattice magnetizations. The measurements were performed with an incident laser fluence of 4.4 mJ cm⁻² and a sample temperature of 83 K, which is well below $T_M = 250$ K.

First, the net magnetizations of both sublattices rapidly decrease. However, whereas the net magnetization of Fe has collapsed within

¹Radboud University Nijmegen, Institute for Molecules and Materials, Heyendaalseweg 135, 6525 AJ Nijmegen, The Netherlands. ²Helmholtz-Zentrum Berlin für Materialien und Energie, BESSY II, Albert-Einstein-Strasse 15, 12489 Berlin, Germany. ³SLAC National Accelerator Laboratory, Menlo Park, California 94025, USA. ⁴Department of Physics, University of York, York YO10 5DD, UK. ⁵College of Science and Technology, Nihon University, 7-24-1 Funabashi, Chiba, Japan. ⁶PRESTO, Japan Science and Technology Agency, 4-1-8 Honcho Kawaguchi, Saitama, Japan.

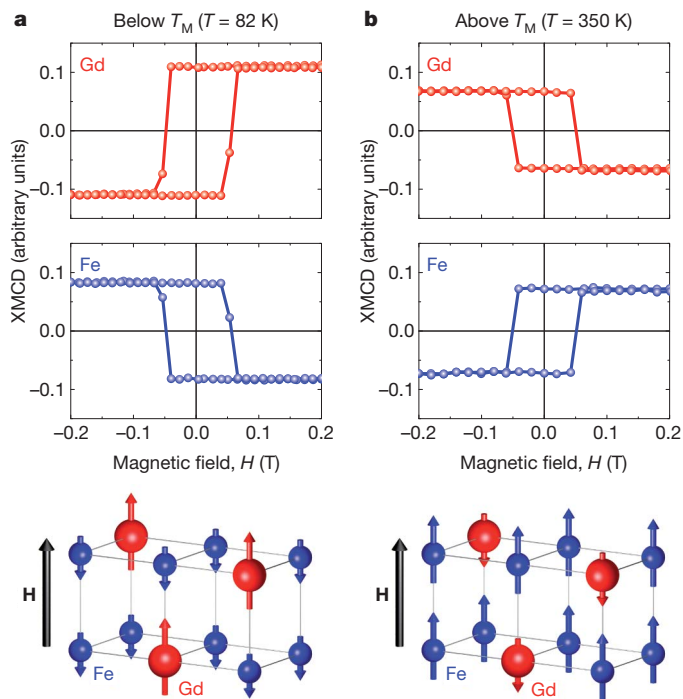


Figure 1 | Ferrimagnetic alignment of the Fe and Gd magnetic moments as measured by element-specific XMCD hysteresis. **a, b, Top,** XMCD signals measured at the Fe and Gd absorption edges as a function of applied magnetic field below **(a)** and above **(b)** the magnetization compensation temperature (T_M), demonstrating the ferrimagnetic alignment of the Fe and Gd magnetic moments. **a, b, Bottom,** a generic ferrimagnet, showing the alignment of the magnetic moments of the constituent sub-lattices with respect to the external magnetic field, H .

300 fs, the demagnetization of Gd takes as long as 1.5 ps. Remarkably, in spite of the exchange coupling between the rare earth and transition metal sublattices, they apparently lose their net magnetizations independently, as would be the case for two decoupled transition metal and rare earth ferromagnets^{13,14}. To retrieve the time constants of the involved processes, we have used a double exponential fit function convoluted with the time resolution of the experiment of 100 fs,

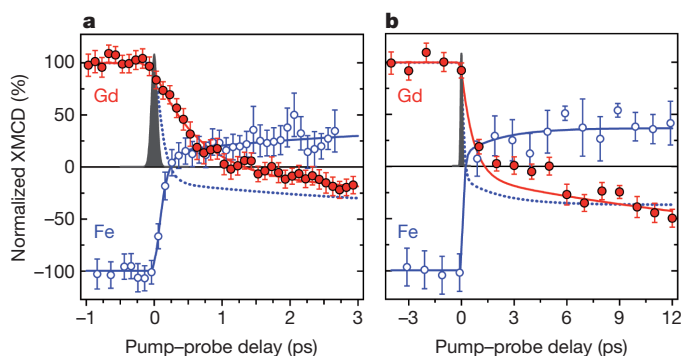


Figure 2 | Element-resolved dynamics of the Fe and Gd magnetic moments measured by time-resolved XMCD with femtosecond time-resolution.

a, Transient dynamics of the Fe (open circles) and Gd (filled circles) magnetic moments measured within the first 3 ps. b, As a but on a 12 ps timescale. Error bars of the experimental data represent the statistical standard error. The measurements were performed at a sample temperature of 83 K for an incident laser fluence of 4.4 mJ cm^{-2} . Experimental time resolution of 100 fs is depicted by the solid Gaussian profile. The solid lines are fits according to a double exponential fit function (Supplementary Information). The dashed line in both panels depicts the magnetization of the Fe sublattice taken with the opposite sign (that is, opposite with respect to the sign of the measured Fe data).

depicted by the Gaussian curve in Fig. 2 (see Supplementary Information section 3). We find a time constant $\tau_{\text{Fe}} = 100 \pm 25 \text{ fs}$ for the Fe and $\tau_{\text{Gd}} = 430 \pm 100 \text{ fs}$ for the Gd magnetic moment, and thus a ratio $\tau_{\text{Gd}}/\tau_{\text{Fe}} \approx 4$, characterizing the fast initial drop in the transient dichroic signal. Note that the laser-induced dynamics studied here rely on crossing the compensation temperature T_M and thus are fundamentally different from the laser-induced demagnetization of pure Fe and Gd that rely on crossing the Curie point T_C (refs 15, 16).

Second, the magnetizations of both sublattices switch their directions by crossing the zero signal level and rebuilding their net magnetic moments. Up to 10 ps, the Gd- and Fe-sublattices show distinctly different switching dynamics. Even more surprisingly, within the time-scale between the zero crossings of the Fe and Gd moments (that is, between 300 fs and 1.5 ps), the net Fe and Gd moments are parallel aligned along the z axis despite antiferromagnetic coupling of the spins in the ground state. Note that the net Fe and Gd moments in the transient ferromagnet-like state are reaching rather large values, up to 25% of the equilibrium magnetization. This, together with the substantial laser-induced increase in temperature, indicates a rather strong transient parallel alignment of the Fe and Gd moments. All these observations mean that we have entered a thus far unexplored regime of magnetization dynamics triggered by an ultrashort stimulus, where two exchange-coupled magnetic sublattices are not in equilibrium with each other, show different magnetization dynamics and store different amounts of energy. Consequently, the concept of a magnon (a quantized collective excitation of spins) in such a non-equilibrium ferrimagnetic state should be re-examined, as this state precedes the establishment of the collective Gd-Fe excitations and magnetic resonances in this material.

To further investigate the effect of laser excitation on the degree of switching, we have also studied the dependence of the Fe and Gd dynamics on the laser fluence. As shown in Supplementary Fig. 3, we observe that slightly decreasing the fluence from 4.4 to 4 mJ cm^{-2} leads to longer but still distinct switching times for Fe and Gd. This results in a longer lived transient ferromagnetic-like state, which spans the time range from 700 fs to about 4 ps for this lower fluence.

To obtain a better understanding of the origin of such strongly non-equilibrium spin dynamics, we have developed a model of a ferrimagnet comprising 10^6 localized atomistic exchange-coupled spins and performed numerical simulations of the dynamics after ultrashort laser excitation (Supplementary Information section 4). The model takes into account realistic magnetic moments for Gd and Fe as well as the exchange constants extracted from experimentally measured temperature dependencies of the sublattice magnetizations. In particular, we used an effective Fe–Gd exchange constant of $4.77 \times 10^{-21} \text{ J per spin}$ ($\sim 140 \text{ fs}$). Following ref. 17, we couple the spin system to the electron temperature, which is calculated using the so-called two-temperature model¹⁸.

Figure 3 shows the results of the simulations when applying a heat pulse with a maximum electron temperature of 1,492 K. First, the time evolution of the sublattice magnetization agrees very well with the experiments, and qualitatively reproduces the timescales for the demagnetization of each sublattice. The time required for the disappearance of the net magnetizations of the sublattices is found to be proportional to the ratio μ/λ , where μ and λ are respectively the magnetic moment of the ion and the damping constant of the sublattice. Second, the ferromagnetic-like state is also reproduced, in a time window close to that observed experimentally. In addition, the reversal of the sublattice magnetizations is found to occur via the mechanism of linear reversal¹³, that is, no transverse moment is observed. Note that even making the Gd–Gd exchange interaction in the simulations as strong as the Fe–Fe interaction does not lead to qualitative changes of the dynamics of the Fe and Gd sublattices (Supplementary Information section 5). Moreover, for the sake of argument the model ignores any differences in the electron temperature and the damping constants

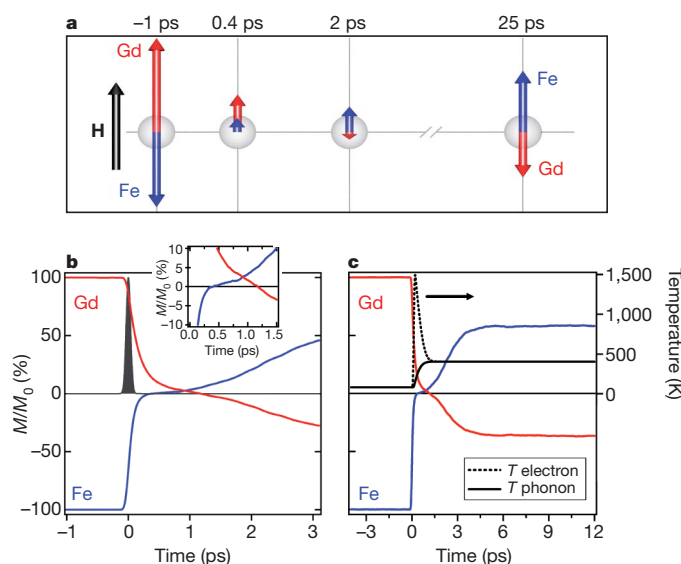


Figure 3 | Computed time-resolved dynamics of the Fe and Gd magnetic moments from localized atomistic spin model. **a**, Cartoon-like illustration of the non-equilibrium dynamics of the Fe and Gd magnetizations with respect to an external magnetic field H . The lengths of the arrows are scaled to the magnitude of the transient XMCD signals shown in Fig. 2. **b**, **c**, Simulated dynamics for the first 3 ps (**b**) and the first 12 ps (**c**) after laser excitation. The calculations were performed for a peak electronic temperature of 1,492 K with the corresponding transient electronic and phononic temperatures shown in **c**. The transient magnetization changes are normalized to magnetization values at negative delays, that is, to equilibrium values. As is clearly seen, the demagnetization of the Fe is much faster than that of the Gd (see inset in **b**; axes same as main panel). For a time of ~ 0.5 ps, we observe a parallel alignment of magnetizations of the sublattices. The agreement with the experimental data in Fig. 2 is qualitatively excellent.

for Gd and Fe ($\lambda_{\text{Fe}} = \lambda_{\text{Gd}} = 0.05$). However, even after such simplifications a good agreement between the experiment and the simulations is observed. This is a strong indication that the novel magnetization dynamics reported here are an intrinsic property of the spins in a ferrimagnet excited by an ultrashort stimulus.

Both the experiments and the simulations show that the ferromagnetic-like state emerges owing to the substantially different dynamics of the transition metal and rare earth sublattices—in particular, the fact that the transition metal reaches the state with zero net magnetization much faster than the rare earth component. The dynamics of the Fe spins in the following time domain occur on the background of a reducing magnetization of the rare earths. The exchange interaction between the Gd and Fe can flip an Fe spin when a Gd spin is reversed. As the exchange is antiferromagnetic, such a process will promote a growth of the net Fe magnetization in the direction parallel to the remaining magnetization of Gd. The simulations indeed confirm that the growth of the Fe magnetization in this time domain occurs with a speed similar (only slightly lower) to that at which the Gd magnetization decreases (Fig. 3b inset).

To conclude, our findings provide unexpected new insights into the fundamentals of ferrimagnetism, showing that two magnetic sublattices may have totally different spin dynamics even on a timescale much longer than the characteristic time of the exchange interaction between them. In the newly discovered transient ferromagnetic-like state, the magnetic system stores a large amount of energy in the intra- and inter-sublattice exchange interactions. Thus it is reasonable to hypothesize that the much weaker interaction of the spins with an external magnetic field hardly influences the spin dynamics in this ultrafast regime, leading to novel switching scenarios. The discovery of these dynamics is important for both the understanding of the physics of ultrafast magnetic phenomena on the timescale of the

exchange interaction, and for the establishment of the fundamental limits on the speed of magnetic recording and information processing.

METHODS SUMMARY

Element-specific hysteresis curves were measured in transmission by setting the X-ray photon energy at the maximum absorption edge (L_3 edge of Fe and M_5 edge of Gd) and sweeping the external magnetic field (which is orientated normal to the sample surface) over ± 0.5 T. The hysteresis was measured at a fixed X-ray light helicity.

Time-resolved XMCD measurements were performed in transmission using 60-fs laser pulses at a wavelength of 800 nm to photo-excite the sample, and using circularly polarized 100-fs X-ray pulses to probe independently the dynamics of the Fe and Gd magnetic moments. The X-ray photon energy was centred at the maximum absorption edge of Fe (L_3) and Gd (M_5) and the laser-induced changes in transmission were measured for opposite orientations of the external magnetic field (± 0.5 T) at a fixed X-ray light helicity. Using a gated detection system, we could record the transient evolution of the pumped (in the presence of laser excitation) and un-pumped (in absence of laser excitation) XMCD signals as a function of pump-probe delay.

For the atomistic spin simulations, the dynamics of the spin system are described using the Landau–Lifshitz–Gilbert (LLG) equation with Langevin dynamics¹⁷. The model treats GdFeCo as a two-sublattice system with a Heisenberg type of exchange. FeCo is represented by a single generic transition metal sublattice. The exchange constants used in the simulations were obtained by fitting the static, temperature-dependent XMCD measurements for the Fe and Gd sublattices. To simulate the effect of the laser excitation, we couple the spin system to the electron temperature calculated using the two-temperature model¹⁸.

Full Methods and any associated references are available in the online version of the paper at www.nature.com/nature.

Received 13 September 2010; accepted 1 February 2011.

Published online 30 March 2011.

1. Stöhr, J. & Siegmann, H. C. *Magnetism: From Fundamentals to Nanoscale Dynamics* (Springer, 2006).
2. Weiss, P. L'hypothèse du champ moléculaire et la propriété ferromagnétique. *J. Phys. (Paris)* **6**, 661–689 (1907).
3. Neel, L. Influence de fluctuations du champ moléculaire sur les propriétés magnétiques des corps. *Ann. Phys. (Paris)* **17**, 5–9 (1932).
4. Neel, L. Magnetism and local molecular field. *Science* **174**, 985–992 (1971).
5. Beaurepaire, E., Merle, J.-C., Daunois, A. & Bigot, J.-Y. Ultrafast spin dynamics in ferromagnetic nickel. *Phys. Rev. Lett.* **76**, 4250–4253 (1996).
6. Kirilyuk, A., Kimel, A. V. & Rasing, Th. Ultrafast optical manipulation of magnetic order. *Rev. Mod. Phys.* **82**, 2731–2784 (2010).
7. Gurevich, A. G. & Melkov, G. A. *Magnetization Oscillations and Waves* (CRC, 1996).
8. Aeschlimann, M., Vaterlaus, A., Lutz, M., Stambanoni, M. & Maier, F. Ultrafast thermomagnetic writing processes in rare-earth transition-metal thin films. *J. Appl. Phys.* **67**, 4438–4440 (1990).
9. Stanciu, C. D. *et al.* Subpicosecond magnetization reversal across ferrimagnetic compensation points. *Phys. Rev. Lett.* **99**, 217204 (2007).
10. Stanciu, C. D. *et al.* Ultrafast spin dynamics across compensation points in ferrimagnetic GdFeCo: the role of angular momentum compensation. *Phys. Rev. B* **73**, 220402(R) (2006).
11. Stamm, C. *et al.* Femtosecond modification of electron localization and transfer of angular momentum in nickel. *Nature Mater.* **6**, 740–743 (2007).
12. Khan, S. *et al.* Femtosecond undulator radiation from sliced electron bunches. *Phys. Rev. Lett.* **97**, 074801 (2006).
13. Kazantseva, N. *et al.* Linear and elliptical magnetization reversal close to the Curie temperature. *Europhys. Lett.* **86**, 27006 (2009).
14. Koopmans, B. *et al.* Explaining the paradoxical diversity of ultrafast laser-induced demagnetization. *Nature Mater.* **9**, 259–265 (2010).
15. Bartelt, A. F. *et al.* Element-specific spin and orbital momentum dynamics of Fe/Gd multilayers. *Appl. Phys. Lett.* **90**, 162503 (2007).
16. Wietstruck, M. *et al.* Hot electron driven enhancement of spin-lattice coupling in 4f ferromagnets observed by femtosecond x-ray magnetic circular dichroism. Preprint at (<http://arxiv.org/abs/1010.1374>) (2010).
17. Kazantseva, N. *et al.* Slow recovery of the magnetization after a sub-picosecond heat pulse. *Europhys. Lett.* **81**, 27004 (2008).
18. Anisimov, S. I., Kapeliovich, B. L. & Perelman, T. L. Electron emission from metal surfaces exposed to ultrashort laser pulses. *Sov. Phys. JETP* **39**, 375–377 (1974).

Supplementary Information is linked to the online version of the paper at www.nature.com/nature.

Acknowledgements We acknowledge technical support provided by R. Mitzner, K. Hollmack and T. Quast during the slicing measurements. We thank F. Radu and R. Abrudan for their support and help with the static XMCD measurements as well as for discussions. This work was supported by the European Community's Seventh Framework Programme FP7/2007-2013 (grants NMP3-SL-2008-214469

(UltraMagnetron) and 214810 (FANTOMAS) as well as grant no. 226716), the Foundation for Fundamental Research on Matter (FOM), the Netherlands Organization for Scientific Research (NWO), the Nihon University Strategic Projects for Academic Research and the US Department of Energy under contract DE-AC02-76SF00515.

Author Contributions I.R., A.V.K., A.K. and Th.R. designed and coordinated the project; I.R., K.V., C.S. and T.K. performed the measurements; C.S., T.K., N.P. and H.A.D. developed the femtoslicing facility at BESSY II Berlin; I.R. and K.V. performed the data analysis; T.A.O., J.B., R.F.L.E. and R.W.C. developed the atomistic model and performed

the calculations; A.T. and A.I. grew and optimized the samples; and I.R. and A.V.K. coordinated the work on the paper. All the authors contributed to the writing of the manuscript.

Author Information Reprints and permissions information is available at www.nature.com/reprints. The authors declare no competing financial interests. Readers are welcome to comment on the online version of this article at www.nature.com/nature. Correspondence and requests for materials should be addressed to I.R. (i.radu@science.ru.nl) and A.V.K. (a.kimel@science.ru.nl).

METHODS

The studied samples are amorphous thin films of $\text{Gd}_{25}\text{Fe}_{65.6}\text{Co}_{9.4}$ of 30 nm thickness which have been deposited by magnetron sputtering on a free-standing Al foil of 500 nm thickness. To avoid oxidation of the GdFeCo layer, Si_3N_4 films of 100 nm and 60 nm thickness were used as buffer and capping layers, respectively. The films exhibit an out-of-plane magnetic anisotropy as deduced from element-specific hysteresis (Fig. 1).

Static and dynamic XMCD measurements have been performed in transmission for opposite orientations of the external magnetic field (± 0.5 T) and at a fixed X-ray light helicity. The magnetic field is oriented perpendicular to the sample and parallel with the X-ray propagation direction. The element-specific hysteresis curves have been recorded by setting the X-ray photon energy at the maximum absorption edge (L_3 edge of Fe and M_5 edge of Gd) and sweeping the external magnetic field between ± 0.5 T.

The time-resolved XMCD measurements have been performed by exciting the sample with 60 fs laser pulses of 800 nm wavelength at a repetition rate of 3 kHz and probing the subsequent dynamics with 100 fs circularly polarized X-ray pulses. By setting the X-ray photon energy at the maximum absorption edge of Fe (L_3 edge) and Gd (M_5 edge) we could disentangle the dynamics of the Fe and Gd magnetic moments. The typical size of the laser beam in focus was 0.8×0.4 mm that led to an incident laser fluence of 4.4 mJ cm^{-2} . The X-ray beam size was 0.3×0.1 mm. The laser-induced changes of X-ray transmission were measured for opposite orientations of the magnetic field using an Si avalanche photodiode and a gated boxcar detection system. The time evolution of the pumped (in the presence of laser excitation) and un-pumped (in absence of laser excitation) signals have been recorded as a function of pump–probe delay. The dynamic XMCD signals have been obtained from the difference of the laser-induced absorption changes measured for opposite magnetic fields. In the main paper we show the ratio of the pumped and un-pumped XMCD curves. The time-resolved XMCD measurements have been performed at a sample temperature of 83 K.

To fit the time-resolved XMCD data, we have used a double-exponential fit function convoluted with the time resolution of the measurement:

$$f(t) = G(t) * [A - B \times (1 - \exp(-t/\tau_1)) - C \times (1 - \exp(-t/\tau_2))]$$

with $G(t)$ describing the Gaussian function that accounts for the time resolution of 100 fs, A representing the value of the transient signal at negative delays, τ_1 and τ_2 the time constants characterizing the two processes—the initial rapid drop and the slower remagnetization in the opposite magnetization direction—describing the temporal evolution of the data, and B and C are exponential amplitudes. Both the static and dynamic XMCD measurements have been performed at the femtosecond facility at BESSY II Berlin

The dynamics of the spin system are described using the Landau-Lifshitz-Gilbert (LLG) equation with Langevin dynamics, which is a stochastic differential equation with multiplicative noise. The stochastic term augments the local field H_i to incorporate thermal fluctuations. The model uses a numerical solution of the LLG equation:

$$\frac{\partial \mathbf{S}_i}{\partial t} = -\frac{\gamma_i}{(1 + \lambda_i^2)\mu_i} \{ \mathbf{S}_i \times [\mathbf{H}_i + \lambda_i \mathbf{S}_i \times \mathbf{H}_i] \} \quad (1)$$

Here S_i is the spin at the atomic site i , which is normalized to unity, γ_i is the gyromagnetic ratio associated with the spin at site i and μ_i is the magnetic moment associated with each species. H_i is the effective field at each site, which includes contributions, determined by our Hamiltonian, which we choose to be of the generic Heisenberg form, given by:

$$E = -\sum_{\langle ij \rangle} J_{ij} \mathbf{S}_i \cdot \mathbf{S}_j - \sum_i d_i S_i^z - \sum_i \mu_i \mathbf{B} \cdot \mathbf{S}_z \quad (2)$$

Here J_{ij} is the exchange constant between neighbouring spins, d_i is the uniaxial anisotropy energy per spin and B is the magnetic field. The field at each site is then given by:

$$\mathbf{H}_i = -\frac{\partial E_i}{\partial \mathbf{S}_i} \quad (3)$$

which leads to the expression for the fields:

$$\mathbf{H}_i = \sum_{mn} \mathbf{S}_j + d_i S_i^z + \mu_i \mathbf{B} \quad (4)$$

This field must be evaluated for each spin at each step of the numerical integration. We utilize the Heun method for the numerical integration, which is a second order predictor-corrector method.

For the specific problem of our LLG equation for atomistic spins, we augment equation (3) by adding on the thermal term giving the local field in the form:

$$H_i = -\frac{\partial E_i}{\partial \mathbf{S}_i} + \boldsymbol{\zeta}_i \quad (5)$$

with the stochastic term, $\boldsymbol{\zeta}_i$, having the properties:

$$\langle \zeta_i^a(t) \zeta_j^b(t') \rangle = 2\delta_{ij} \delta_{ab} (t - t') \frac{\lambda_i k_B T \mu_i}{\gamma_i} \quad (6)$$

and

$$\langle \zeta(t) \rangle = 0 \quad (7)$$

The equation of motion is solved for each spin at each time step. We use an f.c.c. lattice randomly populated by transition metal and rare earth spins, for which we use a uniform random number generator.

The longitudinal relaxation calculations are carried out as follows. Spins are initialized in the same direction and the temperature set to the required value. The evolution of the spin system is calculated by direct numerical integration of the coupled equations of motion. The temporal variation of the magnetization is calculated until equilibrium is reached.

For the switching simulations, the system is subjected to a time varying temperature associated with the conduction electron heat bath. The electron temperature is calculated from the two temperature model¹⁸:

$$\begin{aligned} C_e \frac{\partial T_e}{\partial t} &= -\nabla \cdot \mathbf{Q}_e - G(T_e - T_l) + S(\mathbf{r}, t) \\ \tau_e \frac{\partial \mathbf{Q}_e}{\partial t} + \mathbf{Q}_e &= -K_e \nabla T_e \\ C_l \frac{\partial T_l}{\partial t} &= -\nabla \cdot \mathbf{Q}_l + G(T_e - T_l) \\ \tau_l \frac{\partial \mathbf{Q}_l}{\partial t} + \mathbf{Q}_l &= -K_l \nabla T_l \end{aligned} \quad (8)$$

Here C_e is the electron specific heat capacity, C_l is the lattice/phonon specific heat capacity, and T_e and T_l are the electron and lattice temperatures, respectively. \mathbf{Q}_e and \mathbf{Q}_l are the heat flux vectors through the electron and lattice systems respectively and are (in general) dependent on the position within the body. G is the electron–phonon coupling factor, τ_e and τ_l are the electron and phonon energy relaxation times, respectively. K_e and K_l are the thermal conductivity constants of the electron and phonon systems, respectively. We assume uniform heating throughout the sample and a Gaussian laser pulse, which reduces equations (8) to only the first and third equation. This can then be solved using direct numerical integration with a first order Euler scheme.

The values of the physical quantities used in this manuscript are summarized as follows. Fe–Fe exchange, $J_{\text{Fe–Fe}} = 2.835 \times 10^{-21}$ J per link. Gd–Gd exchange, $J_{\text{Gd–Gd}} = 1.26 \times 10^{-21}$ J per link. Fe–Gd exchange, $J_{\text{Fe–Gd}} = -1.09 \times 10^{-21}$ J per link. $\alpha_{\text{Fe}} = \alpha_{\text{Gd}}$, for which we use 0.05. Though the qualitative result does not change with the reversal, the timescale will vary. Gyromagnetic ratios, $\gamma_{\text{Fe}} = \gamma_{\text{Gd}} = \gamma$. Magnetic moment of Fe $\mu_{\text{Fe}} = 1.92 \mu_B$. Magnetic moment of Gd $\mu_{\text{Gd}} = 7.63 \mu_B$. Time step $\Delta t_{\text{real}} = 0.1$ fs. Anisotropy constant $d_i = 0.807246 \times 10^{-23}$ J per spin for both the Fe and the Gd.